

# $N_4H_9Cu_7S_4$ : A Hydrazinium-Based Salt with a Layered $Cu_7S_4^-$ Framework

David B. Mitzi\*

IBM T. J. Watson Research Center, P.O. Box 218, Yorktown Heights, New York 10598

Received November 9, 2006

Crystals of a hydrazinium-based copper(I) sulfide salt,  $N_4H_9Cu_7S_4$  (**1**), have been isolated by an ambient temperature solution-based process. In contrast to previously reported hydrazinium salts of main-group metal chalcogenides, which consist of isolated metal chalcogenide anions, and  $ACu_7S_4$  ( $A = NH_4^+$ ,  $Rb^+$ ,  $Tl^+$ ,  $K^+$ ), which contains a more three-dimensional  $Cu_7S_4^-$  framework with partial Cu-site occupancy, the structure of **1** [ $P21$ ,  $a = 6.8621(4)$  Å,  $b = 7.9851(4)$  Å,  $c = 10.0983(5)$  Å,  $\beta = 99.360(1)^\circ$ ,  $Z = 2$ ] is composed of extended two-dimensional  $Cu_7S_4^-$  slabs with full Cu-site occupancy. The  $Cu_7S_4^-$  slabs are separated by a mixture of hydrazinium and hydrazine moieties. Thermal decomposition of **1** into copper(I) sulfide proceeds at a significantly lower temperature than that observed for analogous hydrazinium salts of previously considered metal chalcogenides, completing the transition at temperatures as low as 120 °C. Solutions of **1** may be used in the solution deposition of a range of Cu-containing chalcogenide films.

## Introduction

Hydrazine-based metal chalcogenide salts have recently been shown to serve as precursors for the solution-based film deposition of high-mobility n- and p-type semiconductors.<sup>1–5</sup> Selected main-group metal sulfides, selenides, and tellurides dissolve in hydrazine/chalcogen mixtures at room temperature. Evaporation of the hydrazine solvent leads to formation of the salt precursors, with hydrazinium cations charge-balancing isolated anionic metal chalcogenide moieties [e.g.,  $(N_2H_5)_4Sn_2S_6$ ,  $(N_2H_4)_3(N_2H_5)_4Sn_2Se_6$ , and  $(N_2H_5)_4Ge_2Se_6$ ]. For ZnTe, rather than an ionic salt, the resulting precursor consists of extended ZnTe chains with two covalently bonded hydrazine molecules per Zn atom.<sup>6</sup> Despite being covalent,  $(N_2H_4)_2ZnTe$  is still soluble in hydrazine at room temperature and can therefore also effectively be used for solution-based film deposition. For both ionic and covalent precursors, the low-temperature solution-based nature of the hydrazine-precursor approach renders the process attractive for potential

use in a number of low-cost and/or large-area electronic applications.

While the previously considered examples of hydrazinium-based precursors have primarily involved main-group metal chalcogenides, there are a number of other important systems that require incorporation of a transition metal.  $CuInSe_2$ , for example, is used as the active absorber layer in high-efficiency thin-film solar cells. Typically, the chalcopyrite material is deposited by evaporation or sputtering.<sup>7–9</sup> However, the development of a low-cost, high-throughput, solution-based film deposition technique would be highly desirable to reduce the cost of the resulting devices. Recently, we described the application of the hydrazine-based precursor approach to the deposition of  $CuInSe_{2-x}S_x$ .<sup>4</sup> The process requires the use of a hydrazine-based precursor of  $Cu_2S$ ,  $N_4H_9Cu_7S_4$ , as well as an analogous  $In_2Se_3$  precursor. The same copper(I) precursor was used to deposit films of  $CuInTe_2$ , with S being replaced by Te during the final heat treatment.<sup>5</sup> In this study, the detailed crystal structure and thermal properties of  $N_4H_9Cu_7S_4$  (**1**) are examined. The structure of **1** is found to be composed of extended  $Cu_7S_4^-$  sheets,

\* To whom correspondence should be addressed. E-mail: dmitzi@us.ibm.com.

- (1) Mitzi, D. B.; Kosbar, L. L.; Murray, C. E.; Copel, M.; Afzali, A. *Nature* **2004**, *428*, 299.
- (2) Mitzi, D. B. *Inorg. Chem.* **2005**, *44*, 3755.
- (3) Mitzi, D. B.; Copel, M.; Chey, S. J. *Adv. Mater.* **2005**, *17*, 1285.
- (4) Milliron, D. J.; Mitzi, D. B.; Copel, M.; Murray, C. E. *Chem. Mater.* **2006**, *18*, 587.
- (5) Mitzi, D. B.; Copel, M.; Murray, C. E. *Adv. Mater.* **2006**, *18*, 2448.
- (6) Mitzi, D. B. *Inorg. Chem.* **2005**, *44*, 7078.

- (7) Tuttle, J. R.; Contreras, M.; Bode, M. H.; Niles, D.; Albin, D. S.; Matson, R.; Gabor, A. M.; Tennant, A.; Duda, A.; Noufi, R. *J. Appl. Phys.* **1995**, *77*, 153.
- (8) Alberts, V.; Chenene, M. L. *Semicond. Sci. Technol.* **2003**, *18*, 870.
- (9) Bhattacharyya, D.; Forbes, I.; Adurodija, F. O.; Carter, M. J. *J. Mater. Sci.* **1997**, *32*, 1889.

separated by a mixture of hydrazinium and hydrazine molecules, making this the first example among the reported structurally characterized hydrazinium-based salts with an extended 2-D metal chalcogenide anion. Additionally, **1** is found to decompose at a substantially lower temperature than previously studied hydrazinium-based precursors, completing the decomposition process to copper(I) sulfide by  $\sim 120^\circ\text{C}$ .

## Experimental Section

**Synthesis of  $\text{N}_4\text{H}_9\text{Cu}_7\text{S}_4$  (**1**).** In an inert atmosphere, 1 mmol of  $\text{Cu}_2\text{S}$  (159 mg; Aldrich, anhydrous, 99.99%) and 2 mmol S (64 mg; Aldrich, 99.998%) are stirred at room temperature with 4 mL of hydrazine (Aldrich, anhydrous, 98%). **Caution:** hydrazine is highly toxic and should be handled with appropriate protective equipment to prevent contact with either the vapors or liquid. The mixture is allowed to stir in a sealed vial for 90 h, yielding an essentially clear yellow solution (a few specks of undissolved black material remain). The solution is then passed through a  $0.2\text{-}\mu\text{m}$  syringe filter into a new vial and evaporated under flowing nitrogen gas, yielding  $\sim 163$  mg of the black crystalline product (0.255 mmol of  $\text{N}_4\text{H}_9\text{Cu}_7\text{S}_4$  or  $\sim 89\%$  yield based on the starting Cu stoichiometry). The powder X-ray diffraction pattern of the product is in good agreement with that expected for **1**. The calculated powder pattern in this case was generated with the Mercury (v 1.3) program (CCDC)<sup>10</sup> and the atomic coordinates of **1** (see discussion of structure below). Chemical analysis (performed in duplicate by Galbraith Laboratories): observed N (8.3%), H (1.3%); calcd for  $\text{N}_4\text{H}_9\text{Cu}_7\text{S}_4$  N (8.78%), H (1.42%).

**Powder X-ray Diffraction.** Powder XRD patterns were collected on a Siemens D5000 diffractometer (Cu  $K\alpha$  radiation) for **1**, as well as for the thermal decomposition product formed upon heating **1** in the thermogravimetric analysis apparatus under flowing nitrogen to various temperatures. The phases present in each thermally decomposed sample were initially identified (e.g.,  $\text{Cu}_2\text{S}$ ) by comparison with powder diffraction file (PDF) cards. Pawley refinement<sup>11</sup> of structural parameters from the full diffraction profile was performed with the Bruker Topas(P) software package (version 2.1) and initial cell constants from the PDF card for chalcocite (33-0490). The peak profiles were fitted by use of a pseudo-Voigt function. The final Pawley refinement  $R_{\text{wp}}$  was 1.59% (goodness of fit = 1.44) for the data in Figure 7b.

**X-ray Crystallography.** A darkly colored, thin platelike  $\text{N}_4\text{H}_9\text{Cu}_7\text{S}_4$  (**1**) crystal, with the approximate dimensions  $0.01\text{ mm} \times 0.3\text{ mm} \times 0.3\text{ mm}$ , was selected under a microscope and attached to the end of a quartz fiber with 5 min epoxy. Intensity data were collected at  $-35^\circ\text{C}$  with a Bruker Smart 1000 diffractometer equipped with a fine focus 2.4 kW sealed tube X-ray source (Mo  $K\alpha$  radiation). A detector distance of approximately 5.0 cm and an exposure time of 14 s/frame were employed for the collection of 2272 frames with increasing  $\omega$ . The increment in  $\omega$  between each frame was  $0.3^\circ$ .

Final unit cell parameters (Table 1) and crystal orientation matrix were obtained by a least-squares fit of 5711 reflections. An empirical absorption correction based on equivalent reflections was applied to the intensity data.<sup>12</sup> The structure was solved and refined

**Table 1.** Crystallographic Data (at 240 K) for **1**

chemical formula	$\text{N}_4\text{H}_9\text{Cu}_7\text{S}_4$
formula weight	638.18
space group	$P2_1$ (No. 4)
$a$ , Å	6.8621(4)
$b$ , Å	7.9851(4)
$c$ , Å	10.0983(5)
$\beta$ , deg	99.360(1)
$V$ , Å <sup>3</sup>	545.96(5)
$Z$	2
$\rho_{\text{calcd}}$ , g/cm <sup>3</sup>	3.882
wavelength, Å	0.710 73 (Mo $K\alpha$ )
absorp. coeff ( $\mu$ ), cm <sup>-1</sup>	141.0
$R_{\text{f}}^a$	0.038
$R_{\text{w}}^b$	0.046

$$^a R_{\text{f}} = \sum(|F_{\text{o}}| - |F_{\text{c}}|) / \sum(|F_{\text{o}}|). \quad ^b R_{\text{w}} = \{ \sum w(|F_{\text{o}}| - |F_{\text{c}}|)^2 / \sum (w|F_{\text{o}}|^2) \}^{1/2}.$$

by use of the NRCVAX 386 PC version program.<sup>13</sup> The Cu, S, and N atoms were located using both direct methods and Fourier difference maps, and the positions were refined with anisotropic thermal parameters. Hydrogen atoms were located from difference maps and fully refined with isotropic thermal parameters. The extra proton on the hydrazine molecule (to yield the hydrazinium cation) was not well localized in the difference maps. It was therefore refined as disordered over the two hydrazine molecules as discussed in the Results and Discussion section. The minimum and maximum peaks in the final difference Fourier maps corresponded to  $-1.7$  and  $1.4\text{ e}/\text{\AA}^3$ . No additional symmetry was detected for the refined structures with the MISSYM program.<sup>14</sup> Attempts to refine the heavy atom (Cu, S, N) site occupancies led to no evidence for vacancies on any of these sites (refined occupancies fell within  $\pm 0.02$  of 1). A complete listing of crystallographic data (in CIF format) is given as Supporting Information.

In addition to the  $-35^\circ\text{C}$  structure of **1** reported here, a similar refinement was performed at room temperature, yielding only slightly shifted (to larger volume) lattice constants relative to the low-temperature data collection:  $a = 6.8662(5)\text{ \AA}$ ,  $b = 7.9892(6)\text{ \AA}$ ,  $c = 10.1313(8)\text{ \AA}$ ,  $\beta = 99.523(1)^\circ$ , and  $V = 548.1(1)\text{ \AA}^3$ . No structural transition was detected upon cooling to temperatures as low as  $-70^\circ\text{C}$ .

**Thermal Analysis.** Thermogravimetric analysis (TGA) scans were performed, on a TA Instruments TGA-2950 system, in a flowing nitrogen atmosphere and with a  $5^\circ\text{C}/\text{min}$  ramp to  $300^\circ\text{C}$ . The thermal analysis apparatus was also used to decompose samples of **1** at selected temperatures at or below  $300^\circ\text{C}$  (in nitrogen atmosphere). Each thermal treatment was based on a  $5^\circ\text{C}/\text{min}$  ramp to the desired temperature, followed by a dwell at the final temperature for 10 min. After thermal decomposition, each sample was examined by X-ray diffraction for phase analysis.

## Results and Discussion

**Crystal Structure.** The phase diagram and crystal chemistry of binary copper(I) sulfides are relatively complex, with at least four well-defined phases in the vicinity of 2 Cu:1 S. Chalcocite,  $\text{Cu}_2\text{S}$ , is found in two forms.<sup>15</sup> The high-temperature form (high-chalcocite;  $P6_3/mmc$ ,  $a = 3.96\text{ \AA}$ ,  $c = 6.72\text{ \AA}$ ,  $Z = 2$ ) exists at temperatures above approximately  $100^\circ\text{C}$  and is composed of a hexagonal-close-packed framework of sulfur atoms, with a highly disordered and likely mobile arrangement of the copper atoms in the

(10) Bruno, I. J.; Cole, J. C.; Edgington, P. R.; Kessler, M. K.; Macrae, C. F.; McCabe, P.; Pearson, J.; Taylor, R. *Acta Crystallogr.* **2002**, *B58*, 389.

(11) Pawley, G. S. *J. Appl. Crystallogr.* **1981**, *14*, 357.

(12) Sheldrick, G. M. SADABS; Institut für Anorganische Chemie der Universität Göttingen: Göttingen, Germany, 1997.

(13) Gabe, E. J.; Le Page, Y.; Charland, J. -P. Lee, F. L.; White, P. S. J. *Appl. Crystallogr.* **1989**, *22*, 384.

(14) Le Page, Y. *J. Appl. Crystallogr.* **1988**, *21*, 983.

(15) Evans, H. T., Jr. *Z. Kristallogr.* **1979**, *150*, 299.

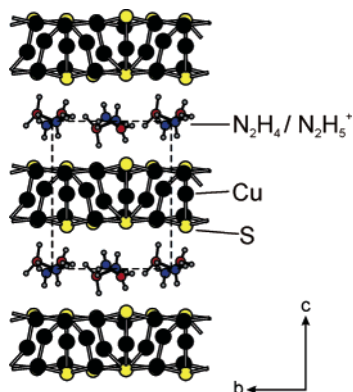


**Figure 1.** Detailed structure of **1** viewed down [100], with unit cell shown (---). For clarity, atoms are represented as spheres, with uniform sizes selected for each atom type. Nitrogen atoms that are refined with a third hydrogen ( $1/2$  occupancy) are depicted in red. Corresponding nitrogen atoms that are part of  $\text{NH}_2$  groups are depicted in blue. Within the  $\text{Cu}_7\text{S}_4^-$  slabs, Cu–Cu bonding is not shown to improve clarity.

interstices. Both the room-temperature form of  $\text{Cu}_2\text{S}$  (low-chalcocite;  $P2_1/c$ ,  $a = 15.246 \text{ \AA}$ ,  $b = 11.884 \text{ \AA}$ ,  $c = 13.494 \text{ \AA}$ ,  $\beta = 116.35^\circ$ ,  $Z = 48$ ) and the slightly copper-deficient compound  $\text{Cu}_{31}\text{S}_{16}$  (djurleite;  $P2_1/n$ ,  $a = 26.897 \text{ \AA}$ ,  $b = 15.745 \text{ \AA}$ ,  $c = 13.565 \text{ \AA}$ ,  $\beta = 90.13^\circ$ ,  $Z = 8$ ), which are often found intermixed or intergrown, are based on the same hexagonal-close-packed sulfur framework as high-chalcocite, with, however, distinct ordered arrangements of the copper atoms in the interstices.<sup>15</sup> Although the copper atoms in the two related compounds generally have two, three, or four sulfur neighbors, the predominant copper coordination is triangular. As for chalcocite, digenite ( $\text{Cu}_{1.8}\text{S}$ ) exists in two modifications.<sup>16,17</sup> Above approximately  $75^\circ\text{C}$ , the high-temperature form (high-digenite;  $Fm\bar{3}m$ ,  $a = 5.57 \text{ \AA}$ ,  $Z = 4$ ) consists of a cubic-close-packed sulfur framework with a fully disordered arrangement of copper atoms filling the interstices, while at room temperature, ordering of the copper atoms gives rise to a superstructure (low-digenite;  $R\bar{3}m$ ,  $a = 3.93 \text{ \AA}$ ,  $c = 48.14 \text{ \AA}$ ,  $Z = 15$ ). The structure of an even more copper-deficient system,  $\text{Cu}_7\text{S}_4$  (anilite;  $Pnma$ ,  $a = 7.89 \text{ \AA}$ ,  $b = 7.84 \text{ \AA}$ ,  $c = 11.01 \text{ \AA}$ ,  $Z = 4$ ), is also based on a cubic-close-packing of sulfur atoms and represents a distinct superstructure of high-digenite.<sup>18</sup> As seen from the above structures, depending on the stoichiometry of the copper sulfide framework, the sulfur atoms may adopt either hexagonal closest packing (chalcocite and djurleite) or cubic closest packing (digenite and anilite). Ordering of the copper atoms in these phases leads to slight displacements of the sulfur atoms with respect to the ideal closest-packed arrangement.

The structure for **1** (Figure 1) consists of well-defined  $\text{Cu}_7\text{S}_4^-$  sheets separated by hydrazinium cations and hydrazine molecules. The extended two-dimensional (2-D) inorganic anion of **1** is distinct from the three-dimensional (3-D) frameworks found in the binary copper sulfides (described

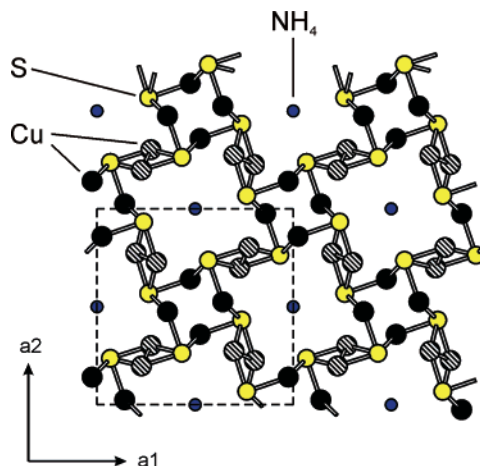


**Figure 2.** Crystal structure of  $\text{NH}_4\text{Cu}_7\text{S}_4$  viewed down [001], with unit cell shown (---).<sup>19</sup> For clarity, atoms are represented as spheres, with uniform sizes selected for each atom type. Partially occupied copper sites are drawn with cross-hatching (fully occupied sites are black-filled). Hydrogen atoms for the  $\text{NH}_4^+$  group are not shown. Within the  $\text{Cu}_7\text{S}_4^-$  framework, Cu–Cu bonding is not shown to improve clarity.

above)<sup>15–18</sup> and in  $(\text{NH}_4)\text{Cu}_7\text{S}_4$ ,<sup>19,20</sup> which contains an anion with nominally the same stoichiometry as for **1**. In  $(\text{NH}_4)\text{Cu}_7\text{S}_4$ , as well as in isotopic  $\text{ACu}_7\text{S}_4$  ( $A = \text{Tl}, \text{Rb}, \text{K}$ ),<sup>21–24</sup>  $\text{Cu}_4\text{S}_4^{4-}$  chains extend along [001], with additional  $\text{Cu}^+$  ions partially occupying sites (occupancy =  $3/4$ ) between the chains and linking them together into a three-dimensional (3-D) structure (Figure 2). Each of these  $\text{ACu}_7\text{S}_4$  ( $A = \text{NH}_4^+$ ,  $\text{Tl}^+$ ,  $\text{Rb}^+$ ,  $\text{K}^+$ ) systems is generally found to be copper-deficient and therefore is better expressed as  $\text{ACu}_{7-x}\text{S}_4$ .<sup>20,23,24</sup> The remaining ammonium (or Tl, Rb, K) cations occupy sites between the  $\text{Cu}_4\text{S}_4^{4-}$  chains, filling channels that extend along [001] (Figure 2).

The 2-D  $\text{Cu}_7\text{S}_4^-$  anions of **1** are in the form of trilayer slabs (Figure 1). The top and bottom layers of the slab can be viewed as a distorted hexagonal  $\text{Cu}_4\text{S}_4^{4-}$  net (Figure 3). The copper atoms in these outer layers are either coordinated to three sulfurs, as in Cu1, Cu5, and Cu4, or to two sulfurs, as for Cu3 (Figure 4a), with Cu–S bond lengths ranging from 2.162 to 2.391  $\text{\AA}$  (shortest bonds involve two-coordinated Cu3). A similar range of Cu–S bond lengths has been reported in chalcocite ( $\text{Cu}_2\text{S}$ ).<sup>15,25</sup> Note that, for Cu3, there is an additional neighboring sulfur with a long Cu3–S2 distance (3.08  $\text{\AA}$ ) (see Figure 3), rendering Cu3 pseudo-3-fold coordinated, similar to the other copper atoms in the outer sheets. Each copper atom also has several interactions of varying length with other copper atoms ( $d_{\text{Cu–Cu}} \geq 2.575 \text{ \AA}$ ) (Figure 4a). For comparison, the Cu–Cu distance in

(16) Donnay, G.; Donnay, J. D. H.; Kullerud, G. *Am. Mineral.* **1958**, *43*, 228.

(17) Will, G.; Hinze, E.; Abdelrahman, A. R. M. *Eur. J. Mineral.* **2002**, *14*, 591.

(18) Koto, K.; Morimoto, N. *Acta Crystallogr.* **1970**, *B26*, 915.

(19) Gattow, G. *Acta Crystallogr.* **1957**, *10*, 549.

(20) Norén, L.; Berger, R.; Lidin, S.; Eriksson, L.; Huster, J.; Petříček, V. *J. Alloys Compd.* **1999**, *288*, 102.

(21) Ohtani, T.; Ogura, J.; Sakai, M.; Sano, Y. *Solid State Commun.* **1991**, *78*, 913.

(22) Ohtani, T.; Ogura, J.; Yoshihara, H.; Yokota, Y. *J. Solid State Chem.* **1995**, *115*, 379.

(23) Whangbo, M.-H.; Canadell, E. *Solid State Commun.* **1992**, *81*, 895.

(24) (a) Li, H.; Mackay, R.; Hwu, S.-J.; Kuo, Y.-K.; Skove, M. J.; Yokota, Y.; Ohtani, T. *Chem. Mater.* **1998**, *10*, 3172. (b) Kuo, Y.-K.; Skove, M. J.; Verebelyi, D. T.; Li, H.; Mackay, R.; Hwu, S.-J.; Whangbo, M.-H.; Brill, J. W. *Phys. Rev. B* **1998**, *57*, 3315.

(25) Evans, H. T., Jr. *Science* **1979**, *203*, 356.



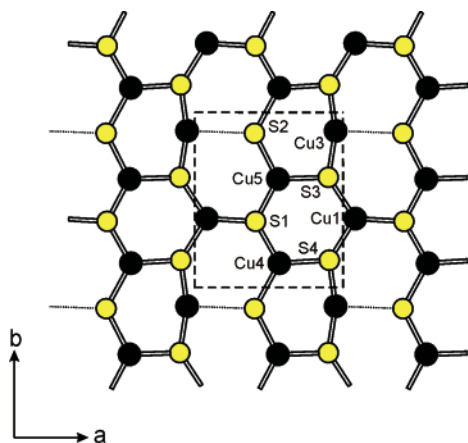


**Figure 3.** Structure of the outer  $\text{Cu}_4\text{S}_4^{4-}$  layer of the  $\text{Cu}_7\text{S}_4^-$  slab from **1** viewed down [001], with unit cell shown (---) and atom labeling indicated. The relatively weak interaction between Cu3 and S2 is denoted by a dotted line. For clarity, atoms are represented as spheres, with uniform sizes selected for each atom type.

copper metal is on the order of  $2.55 \text{ \AA}$ ,<sup>26</sup> suggesting that at least the shortest of these interactions in **1** is significant. The central layer consists entirely of copper atoms (Cu2, Cu6, Cu7), which each coordinate to two sulfurs from the outer layers and a number of other copper atoms (Figure 4b). The copper atoms in the central layer link the two outer sheets together into a 2-D slab with overall thickness of  $\sim 4.15 \text{ \AA}$ . In contrast to the  $\text{ACu}_7\text{S}_4$  salts, all sites in the  $\text{Cu}_7\text{S}_4^-$  moiety for **1** appear to be fully occupied and ordered.

The two independent hydrazine molecules in **1**, N1–N2 and N3–N4, have essentially the same N–N bond length [ $1.46(1)$  and  $1.47(1) \text{ \AA}$ , respectively] and occupy a gallery between the  $\text{Cu}_7\text{S}_4^-$  anions that is  $\sim 5.81 \text{ \AA}$  thick (Figure 1). Each hydrazine molecule has one nitrogen (i.e., N1 and N3; shown in red in Figure 1) that is significantly closer to the plane of the sulfur atoms in the  $\text{Cu}_7\text{S}_4^-$  slab than the corresponding partner nitrogen (i.e., N2 and N4; shown in blue). For N1–N2, the N1 atom is  $\sim 2.39 \text{ \AA}$  from the plane defined by the outermost S1 atoms of the  $\text{Cu}_7\text{S}_4^-$  slab ( $2.63 \text{ \AA}$  distance for N2), while the analogous distance for N3 in the N3–N4 molecule is  $2.42 \text{ \AA}$  ( $2.85 \text{ \AA}$  distance for N4). Given the similarity in the intramolecular N–N bond lengths and closest contact distances to the extended anion, there is no reason to suspect one hydrazine molecule over the other for protonation. For this reason, the extra proton was refined as disordered and equally distributed between N1 and N3.

Hydrogen bonding between hydrazinium cations and metal chalcogenide anions is quite extensive in the previously reported  $(\text{N}_2\text{H}_5)_4\text{Sn}_2\text{S}_6$  salt (the other published example of a sulfur-based hydrazinium salt),<sup>1</sup> with numerous  $\text{N}\cdots\text{S}$  contact distances ranging from  $3.18$  to  $3.28 \text{ \AA}$  (generally multiple short contacts per nitrogen), and nearly linear  $\text{N}-\text{H}\cdots\text{S}$  bond angles ( $\sim 150$ – $170^\circ$ ). The observed hydrogen bonding in **1** is much more limited, perhaps because of the extended 2-D nature of the anion, which provides less structural flexibility than for isolated  $\text{Sn}_2\text{S}_6^{4-}$  anions. For **1**, only two  $\text{N}\cdots\text{S}$  interactions are found with  $\text{N}\cdots\text{S}$  distances

of  $< 3.4 \text{ \AA}$  ( $d_{\text{N1}\cdots\text{S3}} = 3.32 \text{ \AA}$ ,  $d_{\text{N3}\cdots\text{S1}} = 3.35 \text{ \AA}$ ), both of which are significantly longer than those found in the  $(\text{N}_2\text{H}_5)_4\text{Sn}_2\text{S}_6$  salt. Each of these nitrogen atoms (N1 and N3) actually interacts with three sulfurs. For example, N1 has  $\text{N1}\cdots\text{S3}$  [ $d_{\text{N1}\cdots\text{S3}} = 3.32(1) \text{ \AA}$ ,  $\angle\text{N1}-\text{H}\cdots\text{S3} = 110(10)^\circ$ ],  $\text{N1}\cdots\text{S4}$  [ $d_{\text{N1}\cdots\text{S4}} = 3.48(1) \text{ \AA}$ ,  $\angle\text{N1}-\text{H}\cdots\text{S4} = 141(10)^\circ$ ], and  $\text{N1}\cdots\text{S1}$  [ $d_{\text{N1}\cdots\text{S1}} = 3.49(1) \text{ \AA}$ ,  $\angle\text{N1}-\text{H}\cdots\text{S1} = 130(9)^\circ$ ]. The relatively long  $\text{N}\cdots\text{S}$  distances and large deviation of the  $\text{N}-\text{H}\cdots\text{S}$  bond angles from  $180^\circ$  (the  $\text{N}-\text{H}\cdots\text{S}$  distances between hydrogen and sulfur are also large:  $2.6 \leq d_{\text{H}\cdots\text{S}} \leq 3.0$ ) suggest relatively weak  $\text{N}-\text{H}\cdots\text{S}$  hydrogen bonding.<sup>27</sup>

In addition to hydrogen bonding between the hydrazine and hydrazinium moieties and the  $\text{Cu}_7\text{S}_4^-$  anion, there is also significant hydrogen bonding among the hydrazine molecules and hydrazinium cations (as for other hydrazinium salt compounds). In  $(\text{N}_2\text{H}_4)_3(\text{N}_2\text{H}_5)_4\text{Sn}_2\text{Se}_6$ , for example, alternating hydrazinium cations and hydrazine molecules form hydrogen-bonded heptamers, which form short twisted chains among the  $\text{Sn}_2\text{Se}_6^{4-}$  anions.<sup>2</sup> In  $(\text{N}_2\text{H}_5)_4\text{Ge}_2\text{Se}_6$ , the hydrazinium cations form extended hydrogen-bonded chains within the structure.<sup>2</sup> Analogous hydrogen-bonded chains have been observed in  $(\text{N}_2\text{H}_5)\text{Cl}$ ,  $(\text{N}_2\text{H}_5)\text{HC}_2\text{O}_4$ , and  $(\text{N}_2\text{H}_5)\text{H}_2\text{PO}_4$ ,<sup>28–30</sup> with, in each case, hydrogen bonding extending from the  $\text{NH}_3^+$  group of one cation to the  $\text{NH}_2$  group of a neighboring cation (or neutral molecule). The reported  $\text{N}\cdots\text{N}$  hydrogen-bonding distances in the hydrazinium-based salts have generally ranged from  $2.81$  to  $3.14 \text{ \AA}$ .<sup>2,28–30</sup> In **1**, extended hydrogen-bonded chains are observed along [010] (Figure 5), with relatively short  $\text{N}\cdots\text{N}$  distances of  $2.76 \text{ \AA}$  ( $\text{N1}\cdots\text{N3}$ ) and  $2.84 \text{ \AA}$  ( $\text{N1}\cdots\text{N4}$ ). The corresponding bonding angles are  $167^\circ$  ( $\text{N1}-\text{H}\cdots\text{N3}$ ) and  $161^\circ$  ( $\text{N1}-\text{H}\cdots\text{N4}$ ). Note that there are apparent hydrogen-bonding links between adjacent  $\text{NH}_3^+$  groups (shown in red in Figure 5). However, the extra proton positions on these groups are half occupied. Therefore, locally, hydrogen bonding is still most likely occurring between an  $\text{NH}_3^+$  and an  $\text{NH}_2$  group (i.e., one of the two adjacent  $\text{NH}_3^+$  groups with half-occupied H site will have the H site empty). This is particularly likely given the short distance between N1 and N3.

**Thermal Analysis.** A low decomposition temperature (to form the targeted metal chalcogenide) is important with respect to the facile deposition of metal chalcogenide films from a precursor solution on the widest range of substrates.<sup>1–5</sup> For example, polyimide-based substrates (e.g., Kapton) may withstand processing temperatures of as high as  $400 \text{ }^\circ\text{C}$ , while less-expensive plastics such as polyethylene terephthalate (PET), polyethylene naphthalate (PEN), polycarbonate (PC), and polyethersulfone (PES) have glass transitions on the order of  $78$ ,  $120$ ,  $150$ , and  $220 \text{ }^\circ\text{C}$ , respectively.<sup>31</sup> Even if these latter materials are heat-stabilized, they are generally suitable for processing only at temperatures  $< 200 \text{ }^\circ\text{C}$ . Consequently, the decomposition temperature of the hy-

(27) Donohue, *J. Mol. Biol.* **1969**, *45*, 231.

(28) Sakurai, K.; Tomiie, Y. *Acta Crystallogr.* **1952**, *5*, 293.

(29) Nilsson, A.; Liminga, R.; Olovsson, I. *Acta Chem. Scand.* **1968**, *22*, 719.

(30) Liminga, R. *Acta Chem. Scand.* **1965**, *19*, 1629.

(31) MacDonald, W. A. *J. Mater. Chem.* **2004**, *14*, 4.

(26) Pauling, L. *Phys. Rev.* **1938**, *54*, 899.

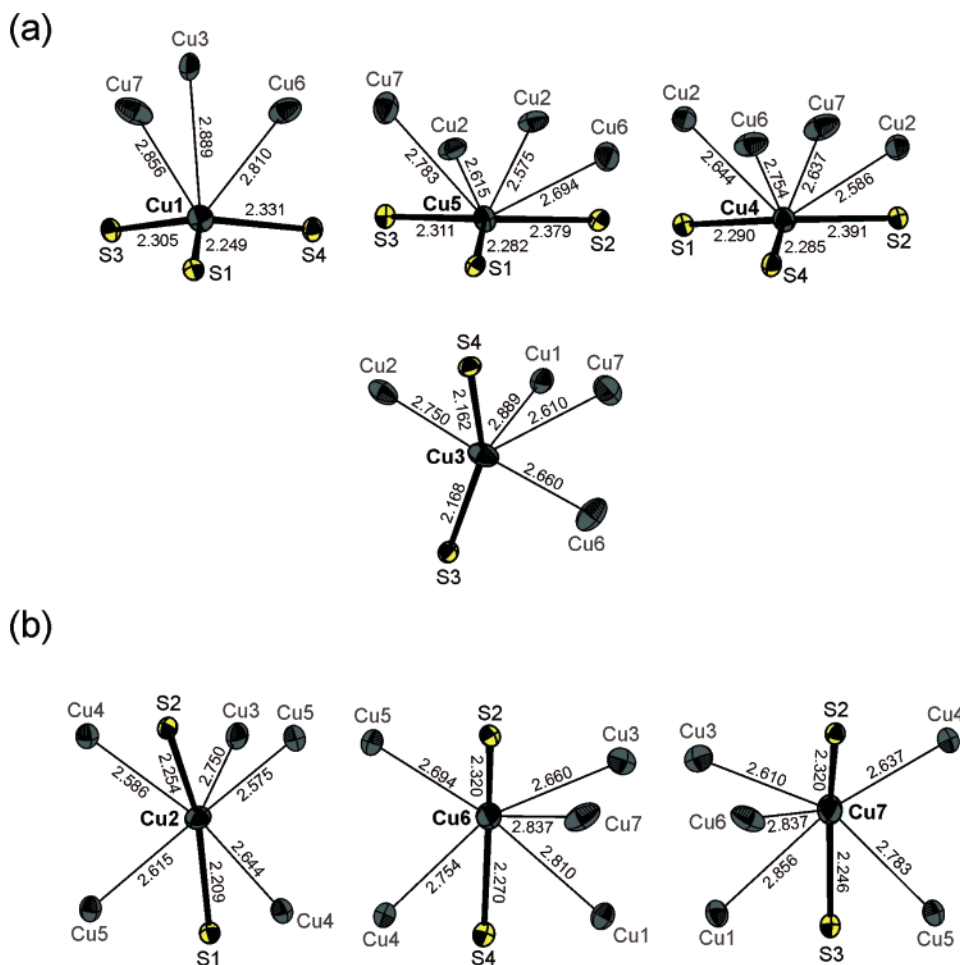


**Figure 4.** Coordination sphere about each copper atom in **1**, with atom labeling and bond lengths (in angstroms) indicated. In panel a, the coordination spheres for the copper atoms in the outer layers of the  $\text{Cu}_7\text{S}_4^-$  slab are presented, while in panel b, the Cu coordinations from the interior layer of the  $\text{Cu}_7\text{S}_4^-$  slab are shown. In each case, only S atoms that are within 2.75 Å of the central Cu atoms are shown. For the neighboring Cu atoms, only those that are within 2.9 Å are considered. The thermal ellipsoids for the Cu and S atoms are drawn at 50% probability.

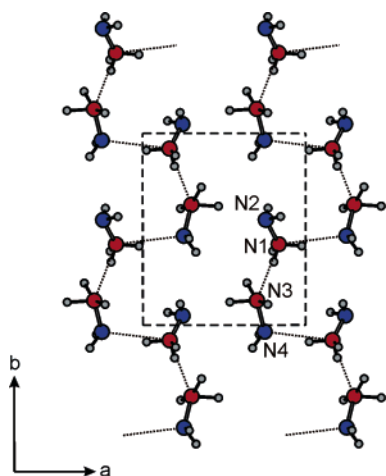


**Figure 5.** Structure of the hydrazine/hydrazinium layer of **1** viewed down [001], with unit cell shown (---). Significant hydrogen-bonding interactions among the hydrazine and hydrazinium moieties are shown with dotted lines. For clarity, atoms are represented as spheres, with uniform sizes selected for each atom type. Nitrogen atoms that are refined with a third hydrogen ( $1/2$  occupancy) are depicted in red. Corresponding nitrogen atoms that are part of  $\text{NH}_2$  groups are depicted in blue.

hydrazinium-based precursors should ideally be below 200 °C to maximize compatibility with the widest range of substrate materials during thin-film deposition.

For the metal chalcogenide hydrazinium-based salts,  $(\text{N}_2\text{H}_4)_x(\text{N}_2\text{H}_5)_y\text{M}^{n+}_2\text{X}_{(2n+y)/2}$ , where M is a metal (e.g., Ge, Sn, In, Sb) with valence  $n$  and X is a chalcogen (e.g., S, Se), decomposition generally occurs by loss of the  $x$  molecules of hydrazine, followed by loss of the protonated hydrazinium moiety and correspondingly  $y/2$  chalcogens.<sup>1–3</sup> This latter transition can occur either as a loss of hydrazine and hydrogen chalcogenide (e.g., as  $\text{H}_2\text{S}$  or  $\text{H}_2\text{Se}$ ) or as a loss of decomposition products of these species (e.g., as  $\text{H}_2$  and S or Se). While, in the case of the sulfide  $(\text{N}_2\text{H}_5)_4\text{Sn}_2\text{S}_6$ , the precursor decomposes at a moderately low temperature ( $\sim 200$  °C),<sup>1</sup> for the corresponding selenides, excess selenium (presumably from the decomposition of  $\text{H}_2\text{Se}$ ) does not evolve from the sample until  $\sim 350$  °C or, in some cases, even higher temperature.<sup>2,3</sup>

Figure 6 shows a typical thermogravimetric analysis (TGA) scan for **1**. Decomposition of the precursor to copper(I) sulfide occurs in essentially a single step and is completed by  $\sim 120$  °C. The overall observed weight loss (12.2%) is in good agreement with that expected for the formation of  $\text{Cu}_2\text{S}$  from **1** (12.7%). X-ray diffraction studies of the final decomposition product (Figure 7) further establish that the precursor is decomposing into chalcocite (although, given structural similarity between chalcocite,  $\text{Cu}_2\text{S}$ , and

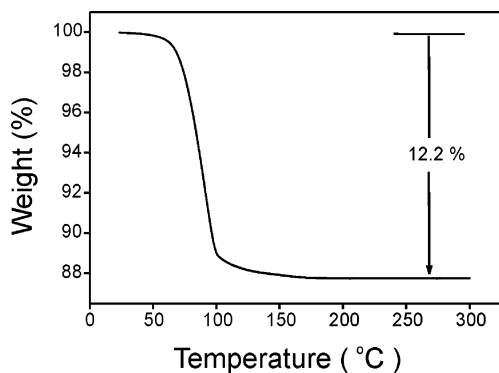


**Figure 6.** Thermogravimetric analysis (TGA) of **1** (5 °C/min ramp rate; nitrogen atmosphere). Weight loss at 270 °C is shown.

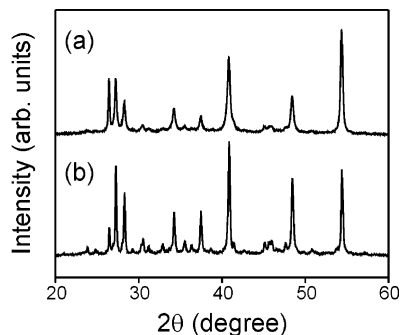


**Figure 7.** Powder X-ray diffraction patterns (Cu  $K\alpha$  radiation) for the decomposition product formed by heating **1** to (a) 125 °C and (b) 300 °C in a nitrogen atmosphere in the TGA apparatus. The diffraction patterns are in good agreement with that expected for chalcocite (PDF 33-0490). A Pawley profile fit of the data in curve b yields (no unindexed reflections) a monoclinic cell with  $a = 15.23(1)$  Å,  $b = 11.88(1)$  Å,  $c = 13.49(1)$  Å, and  $\beta = 116.22(5)^\circ$ .

djurleite,  $\text{Cu}_{31}\text{S}_{16}$ , some impurity of the latter cannot be ruled out). The decomposition process appears to be similar to that observed for  $\text{NH}_4\text{Cu}_7\text{S}_4$ , which decomposes into copper sulfide (apparently digenite) between 120 and 140 °C.<sup>32</sup> The low decomposition temperatures may reflect the relatively weak hydrogen bonding in **1** between the hydrazinium/hydrazine species and the  $\text{Cu}_7\text{S}_4^-$  slabs. Note that in  $\text{NH}_4\text{-Cu}_7\text{S}_4$  there are also relatively long  $\text{N}\cdots\text{S}$  contacts, with the shortest being 3.38 Å.<sup>19</sup>

To verify composition of the decomposition product, films of **1** have also been formed on a thermally oxidized silicon substrate by spin-coating (2000 rpm; processed in nitrogen-filled drybox; decomposition treatment at 200 °C), employing the same solution described in the Experimental Section. The resulting film composition, as determined by Rutherford

backscattering spectroscopy (RBS), is 65.5(5)% Cu and 34.5-(5)% S, which suggests a stoichiometry of  $\text{Cu}_{1.90(5)}\text{S}$ , consistent with the chalcocite stoichiometry to within experimental uncertainty (although the results cannot rule out a slight Cu deficiency).

## Conclusion

The reaction of hydrazine and sulfur with copper(I) sulfide has been used in the deposition of chalcopyrite films, offering some of the highest mobilities achieved to date for spin-coated p-type semiconductors.<sup>4,5</sup> In addition to the realized usefulness of the ternary and quaternary copper-based chalcopyrites in solar cells and other electronic devices, binary copper sulfide materials are potentially interesting in their own right and are being considered for use as solar control coatings (to allow a controlled amount of natural light to enter a building while rejecting as much infrared radiation as possible).<sup>33,34</sup> In this work, we have examined the detailed crystal structure and thermal properties of the copper(I) sulfide salt,  $\text{N}_4\text{H}_9\text{Cu}_7\text{S}_4$  (**1**), which results from the evaporation of the hydrazine/sulfur/copper(I) sulfide solution and which may be used as a precursor for the deposition of copper(I)-containing films.<sup>4,5</sup> In contrast to previously studied hydrazinium precursors of main-group metal chalcogenides,<sup>1,2</sup> which feature isolated metal chalcogenide anions, the metal chalcogenide anion in **1** is in the form of an extended 2-D slab. In **1**, the copper and sulfur sites are fully occupied, while for the analogous more 3-D  $\text{Cu}_7\text{S}_4^-$  anion in  $\text{ACu}_7\text{S}_4$  ( $\text{A} = \text{NH}_4^+$ ,  $\text{Rb}^+$ ,  $\text{Tl}^+$ ,  $\text{K}^+$ ) the Cu sites exhibit partial occupancy. The resulting structure in **1**, with relatively weak hydrogen-bonding between the  $\text{Cu}_7\text{S}_4^-$  anion and hydrazinium/hydrazine species, leads to a very low decomposition temperature for the precursor ( $\sim 120$  °C). The low decomposition temperature is well suited for deposition of copper(I)-containing thin films from solution, even potentially on relatively low-temperature plastics. The resulting films may have utility in the development of solar cell, memory, and other electronic applications.

**Acknowledgment.** I gratefully acknowledge A. Kellock for RBS analysis of the copper sulfide spin-coated films.

**Supporting Information Available:** An X-ray crystallographic file (CIF), containing information for  $\text{N}_4\text{H}_9\text{Cu}_7\text{S}_4$  (**1**). This material is available free of charge via the Internet at <http://pubs.acs.org>.

IC0621291

(32) Boller, H.; Sing, M. *Solid State Ionics* **1997**, 101–103, 1287.

(33) Nair, M. T. S.; Nair, P. K. *Semicond. Sci. Technol.* **1989**, 4, 191.

(34) Nair, M. T. S.; Nair, P. K. *Semicond. Sci. Technol.* **1989**, 4, 599.